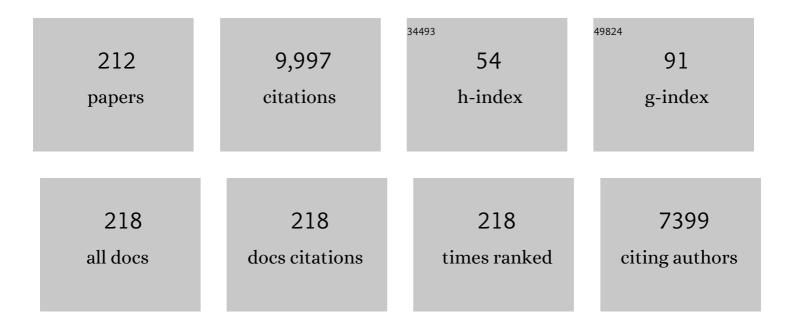
Yanbin Wang

List of Publications by Year in descending order

Source: https://exaly.com/author-pdf/342821/publications.pdf Version: 2024-02-01



YANRIN WANC

| # | Article | IF | CITATIONS |
|----|---|--|--------------------------|
| 1 | A multi-faceted experimental study on the dynamic behavior of MgSiO3 glass in the Earth's deep interior. American Mineralogist, 2022, 107, 1313-1324. | 0.9 | 2 |
| 2 | Sound velocity and compressibility of melts along the hedenbergite (CaFeSi2O6)-diopside (CaMgSi2O6) join at high pressure: Implications for stability and seismic signature of Fe-rich melts in the mantle. Earth and Planetary Science Letters, 2022, 577, 117250. | 1.8 | 7 |
| 3 | Extreme dislocation-mediated plasticity of yttria-stabilized zirconia. Materials Today Physics, 2022, 22, 100588. | 2.9 | 1 |
| 4 | Metamorphism-facilitated faulting in deforming orthopyroxene: Implications for global intermediate-depth seismicity. Proceedings of the National Academy of Sciences of the United States of America, 2022, 119, e2112386119. | 3.3 | 3 |
| 5 | A machine-learning-based method of detecting and picking the first <i>P</i> -wave arrivals of acoustic emission events in laboratory experiments. Geophysical Journal International, 2022, 230, 1818-1823. | 1.0 | 5 |
| 6 | Experimental Evidence Supporting an Overturned Ironâ€Titaniumâ€Rich Melt Layer in the Deep Lunar Interior. Geophysical Research Letters, 2022, 49, . | 1.5 | 5 |
| 7 | Synthesis of the Candidate Topological Compound Ni ₃ Pb ₂ . Journal of the American Chemical Society, 2022, 144, 11943-11948. | 6.6 | 1 |
| 8 | Application of the double-difference relocation method to acoustic emission events in high-pressure deformation experiments. Physics and Chemistry of Minerals, 2022, 49, . | 0.3 | 1 |
| 9 | Shear wave velocities across the olivine – wadsleyite – ringwoodite transitions and sharpness of the 410 km seismic discontinuity. Earth and Planetary Science Letters, 2022, 593, 117690. | 1.8 | 1 |
| 10 | Temperature-dependent hardness of zinc-blende structured covalent materials. Science China Materials, 2021, 64, 2280-2288. | 3.5 | 16 |
| 11 | Plastic Deformation and Strengthening Mechanisms of Nanopolycrystalline Diamond. ACS Nano, 2021, 15, 8283-8294. | 7.3 | 3 |
| 12 | Enhanced visibility of subduction slabs by the formation of dense hydrous phase A. Geophysical Research Letters, 2021, 48, e2021GL095487. | 1.5 | 8 |
| 13 | Observation of 9-Fold Coordinated Amorphous TiO ₂ at High Pressure. Journal of Physical Chemistry Letters, 2020, 11, 374-379. | 2.1 | 10 |
| 14 | Strength and plastic deformation of polycrystalline diamond composites. High Pressure Research, 2020, 40, 35-53. | 0.4 | 4 |
| 15 | Structural Evolution of <mml:math <br="" xmlns:mml="http://www.w3.org/1998/Math/MathML">display="inline"><mml:msub><mml:mrow><mml:mi>SiO</mml:mi></mml:mrow><mml:mrow><mml:mn>2Glass with Si Coordination Number Greater than 6. Physical Review Letters, 2020, 125, 205701.</mml:mn></mml:mrow></mml:msub></mml:math> | nml:1219> <td>nmbranrow><!--</td--></td> | nm b ranrow> </td |
| 16 | High-pressure elastic properties of dolomite melt supporting carbonate-induced melting in deep upper mantle. Proceedings of the National Academy of Sciences of the United States of America, 2020, 117, 18285-18291. | 3.3 | 15 |
| 17 | Toward an international practical pressure scale: A proposal for an IPPS ruby gauge (IPPS-Ruby2020). High Pressure Research, 2020, 40, 299-314. | 0.4 | 143 |
| 18 | Intersectional nanotwinned diamond-the hardest polycrystalline diamond by design. Npj Computational Materials, 2020, 6, . | 3.5 | 20 |

| # | Article | IF | CITATIONS |
|----|--|---------------------|----------------------|
| 19 | Hierarchically structured diamond composite with exceptional toughness. Nature, 2020, 582, 370-374. | 13.7 | 141 |
| 20 | Direct Observation of Room-Temperature Dislocation Plasticity in Diamond. Matter, 2020, 2, 1222-1232. | 5.0 | 48 |
| 21 | Equations of state, phase relations, and oxygen fugacity of the Ru-RuO2 buffer at high pressures and temperatures. American Mineralogist, 2020, 105, 333-343. | 0.9 | 6 |
| 22 | Density of NaAlSi2O6 Melt at High Pressure and Temperature Measured by In-Situ X-ray Microtomography. Minerals (Basel, Switzerland), 2020, 10, 161. | 0.8 | 4 |
| 23 | High-Pressure Sound Velocity Measurements of Liquids Using In Situ Ultrasonic Techniques in a Multianvil Apparatus. Minerals (Basel, Switzerland), 2020, 10, 126. | 0.8 | 12 |
| 24 | The Indo–Eurasia convergent margin and earthquakes in and around Tibetan Plateau. Journal of Mineralogical and Petrological Sciences, 2020, 115, 118-137. | 0.4 | 4 |
| 25 | Unraveling microstrain-promoted structural evolution and thermally driven phase transition in <mml:math xmlns:mml="http://www.w3.org/1998/Math/MathML"> <mml:mrow> <mml:mi>c</mml:mi> <mml:mtext>â^' mathvariant="normal">O <mml:mn>3</mml:mn> </mml:mtext></mml:mrow> <td>۱:mtext> <</td><td>mral:msub><</td></mml:math | ۱ :mte xt> < | mr al: msub>< |
| 26 | Compression of porous aluminum: combined ultrasonic and microtomography measurements with lattice-Boltzmann permeability simulations. High Pressure Research, 2019, 39, 438-456. | 0.4 | 0 |
| 27 | Experimental evidence for wall-rock pulverization during dynamic rupture at ultra-high pressure conditions. Earth and Planetary Science Letters, 2019, 528, 115832. | 1.8 | 14 |
| 28 | Reaction-induced embrittlement of the lower continental crust. Geology, 2019, 47, 235-238. | 2.0 | 37 |
| 29 | An upgraded and integrated large-volume high-pressure facility at the GeoSoilEnviroCARS bending magnet beamline of the Advanced Photon Source. Comptes Rendus - Geoscience, 2019, 351, 269-279. | 0.4 | 5 |
| 30 | Continuous strengthening in nanotwinned diamond. Npj Computational Materials, 2019, 5, . | 3.5 | 32 |
| 31 | A Paris-Edinburgh Cell for High-Pressure and High-Temperature Structure Studies on Silicate Liquids Using Monochromatic Synchrotron Radiation. Minerals (Basel, Switzerland), 2019, 9, 715. | 0.8 | 7 |
| 32 | Approaching diamond's theoretical elasticity and strength limits. Nature Communications, 2019, 10, 5533. | 5.8 | 73 |
| 33 | Strengthening-softening transition in yield strength of nanotwinned Cu. Scripta Materialia, 2019, 162, 372-376. | 2.6 | 24 |
| 34 | Controlling Dimensionality in the Ni–Bi System with Pressure. Chemistry of Materials, 2019, 31, 955-959. | 3.2 | 8 |
| 35 | Pressure-induced structural change in MgSiO ₃ glass at pressures near the Earth's core–mantle boundary. Proceedings of the National Academy of Sciences of the United States of America, 2018, 115, 1742-1747. | 3.3 | 34 |
| 36 | An internally consistent pressure calibration of geobarometers applicable to the Earth's upper mantle using in situ XRD. Geochimica Et Cosmochimica Acta, 2018, 222, 421-435. | 1.6 | 7 |

| # | Article | IF | CITATIONS |
|----|--|-----|-----------|
| 37 | Pressure Dependence of the Liquidus and Solidus Temperatures in the Feâ€P Binary System Determined by In Situ Ultrasonics: Implications to the Solidification of Feâ€P Liquids in Planetary Cores. Journal of Geophysical Research E: Planets, 2018, 123, 1113-1124. | 1.5 | 11 |
| 38 | Dislocation behaviors in nanotwinned diamond. Science Advances, 2018, 4, eaat8195. | 4.7 | 40 |
| 39 | Ultrasonic Velocity of Diopside Liquid at High Pressure and Temperature: Constraints on Velocity Reduction in the Upper Mantle Due to Partial Melts. Journal of Geophysical Research: Solid Earth, 2018, 123, 8676-8690. | 1.4 | 15 |
| 40 | Lower-crustal earthquakes in southern Tibet are linked to eclogitization of dry metastable granulite. Nature Communications, 2018, 9, 3483. | 5.8 | 30 |
| 41 | Thermally Induced Anomaly in the Shear Behavior of Magnetite at High Pressure. Physical Review Applied, 2018, 10, . | 1.5 | 3 |
| 42 | Harry W. Green II (1940–2017). Eos, 2018, 99, . | 0.1 | 0 |
| 43 | Role of plastic deformation in tailoring ultrafine microstructure in nanotwinned diamond for enhanced hardness. Science China Materials, 2017, 60, 178-185. | 3.5 | 21 |
| 44 | Dehydration-driven stress transfer triggers intermediate-depth earthquakes. Nature Communications, 2017, 8, 15247. | 5.8 | 152 |
| 45 | Compressed glassy carbon: An ultrastrong and elastic interpenetrating graphene network. Science Advances, 2017, 3, e1603213. | 4.7 | 110 |
| 46 | Creating Binary Cu–Bi Compounds via High-Pressure Synthesis: A Combined Experimental and Theoretical Study. Chemistry of Materials, 2017, 29, 5276-5285. | 3.2 | 39 |
| 47 | Deep melting reveals liquid structural memory and anomalous ferromagnetism in bismuth. Proceedings of the National Academy of Sciences of the United States of America, 2017, 114, 3375-3380. | 3.3 | 12 |
| 48 | Laboratory earthquakes triggered during eclogitization of lawsonite-bearing blueschist. Earth and Planetary Science Letters, 2017, 459, 320-331. | 1.8 | 88 |
| 49 | A laboratory nanoseismological study on deep-focus earthquake micromechanics. Science Advances, 2017, 3, e1601896. | 4.7 | 30 |
| 50 | Beyond sixfold coordinated Si in SiO ₂ glass at ultrahigh pressures. Proceedings of the National Academy of Sciences of the United States of America, 2017, 114, 10041-10046. | 3.3 | 88 |
| 51 | Local structure of liquid gallium under pressure. Scientific Reports, 2017, 7, 5666. | 1.6 | 19 |
| 52 | Faulting of natural serpentinite: Implications for intermediate-depth seismicity. Earth and Planetary Science Letters, 2017, 474, 138-147. | 1.8 | 42 |
| 53 | Anomalous density and elastic properties of basalt at high pressure: Reevaluating of the effect of melt fraction on seismic velocity in the Earth's crust and upper mantle. Journal of Geophysical Research: Solid Earth, 2016, 121, 4232-4248. | 1.4 | 29 |
| 54 | Coexistence of multiple metastable polytypes in rhombohedral bismuth. Scientific Reports, 2016, 6, 20337. | 1.6 | 16 |

| # | Article | IF | CITATIONS |
|----|---|-----|-----------|
| 55 | Discovery of a Superconducting Cu–Bi Intermetallic Compound by Highâ€Pressure Synthesis. Angewandte Chemie - International Edition, 2016, 55, 13446-13449. | 7.2 | 46 |
| 56 | Sound velocities of aluminumâ€bearing stishovite in the mantle transition zone. Geophysical Research Letters, 2016, 43, 4239-4246. | 1.5 | 16 |
| 57 | Ultrahard stitching of nanotwinned diamond and cubic boron nitride in C2-BN composite. Scientific Reports, 2016, 6, 30518. | 1.6 | 24 |
| 58 | Elastic wave velocities in polycrystalline Mg ₃ Al ₂ Si ₃ O ₁₂ -pyrope garnet to 24 GPa and 1300 K. American Mineralogist, 2016, 101, 991-997. | 0.9 | 22 |
| 59 | The effects of shear deformation on planetesimal core segregation: Results from in-situ X-ray micro-tomography. American Mineralogist, 2016, 101, 1996-2004. | 0.9 | 12 |
| 60 | Imaging in 3D under pressure: a decade of high-pressure X-ray microtomography development at GSECARS. Progress in Earth and Planetary Science, 2016, 3, . | 1.1 | 13 |
| 61 | Experimental evidence supports mantle partial melting in the asthenosphere. Science Advances, 2016, 2, e1600246. | 4.7 | 98 |
| 62 | On velocity anomalies beneath southeastern China: An investigation combining mineral physics studies and seismic tomography observations. Gondwana Research, 2016, 31, 200-217. | 3.0 | 7 |
| 63 | The W-WO2oxygen fugacity buffer (WWO) at high pressure and temperature: Implications forfO2buffering and metal-silicate partitioning. American Mineralogist, 2016, 101, 211-221. | 0.9 | 7 |
| 64 | Ultrahigh-pressure polyamorphism in GeO ₂ glass with coordination number >6. Proceedings of the National Academy of Sciences of the United States of America, 2016, 113, 3436-3441. | 3.3 | 75 |
| 65 | Phase Evolution of Oil Well Cements with Nano-additive at Elevated Temperature/Pressure. ACI Materials Journal, 2016, 113, . | 0.3 | 2 |
| 66 | Acoustic travel time gauges for <i>in-situ</i> determination of pressure and temperature in multi-anvil apparatus. Journal of Applied Physics, 2015, 118, . | 1.1 | 25 |
| 67 | X-ray imaging for studying behavior of liquids at high pressures and high temperatures using Paris-Edinburgh press. Review of Scientific Instruments, 2015, 86, 072207. | 0.6 | 13 |
| 68 | High Pressure Phase-Transformation Induced Texture Evolution and Strengthening in Zirconium Metal: Experiment and Modeling. Scientific Reports, 2015, 5, 12552. | 1.6 | 21 |
| 69 | Nanoarchitectured materials composed of fullerene-like spheroids and disordered graphene layers with tunable mechanical properties. Nature Communications, 2015, 6, 6212. | 5.8 | 57 |
| 70 | High-pressure viscosity of liquid Fe and FeS revisited by falling sphere viscometry using ultrafast X-ray imaging. Physics of the Earth and Planetary Interiors, 2015, 241, 57-64. | 0.7 | 38 |
| 71 | High-pressure, high-temperature plastic deformation of sintered diamonds. Diamond and Related Materials, 2015, 59, 95-103. | 1.8 | 13 |
| 72 | Image-based Stokes flow modeling in bulk proppant packs and propped fractures under high loading stresses. Journal of Petroleum Science and Engineering, 2015, 135, 391-402. | 2.1 | 32 |

| # | Article | IF | CITATIONS |
|----|---|------------|-----------|
| 73 | Crystallographic evidence for simultaneous growth in graphic granite. Gondwana Research, 2015, 27, 1550-1559. | 3.0 | 13 |
| 74 | 18. High-pressure Apparatus Integrated with Synchrotron Radiation. , 2014, , 745-778. | | 0 |
| 75 | High-pressure experimental studies on geo-liquids using synchrotron radiation at the Advanced Photon Source. Journal of Earth Science (Wuhan, China), 2014, 25, 939-958. | 1.1 | 7 |
| 76 | Study of liquid gallium as a function of pressure and temperature using synchrotron x-ray microtomography and x-ray diffraction. Applied Physics Letters, 2014, 105, . | 1.5 | 24 |
| 77 | Ultralow viscosity of carbonate melts at high pressures. Nature Communications, 2014, 5, 5091. | 5.8 | 124 |
| 78 | Phase stability of the <mml:math xmlns:mml="http://www.w3.org/1998/Math/MathML"><mml:mrow><mml:mi>SrMn</mml:mi><mml:msub><mml mathvariant="normal">O<mml:mn>3</mml:mn></mml </mml:msub></mml:mrow>hexagonal perovskite system at high pressure and temperature. Physical Review B, 2014, 90, .</mml:math | :mi 1.1 | 29 |
| 79 | Toward comprehensive studies of liquids at high pressures and high temperatures: Combined structure, elastic wave velocity, and viscosity measurements in the Paris–Edinburgh cell. Physics of the Earth and Planetary Interiors, 2014, 228, 269-280. | 0.7 | 96 |
| 80 | Contrasting sound velocity and intermediate-range structural order between polymerized and depolymerized silicate glasses under pressure. Earth and Planetary Science Letters, 2014, 391, 288-295. | 1.8 | 34 |
| 81 | Experimental investigation of phase transformations of olivine and enstatite at the lower part of the mantle transition zone: Implications for structure of the 660 km seismic discontinuity. Science China Earth Sciences, 2014, 57, 592-599. | 2.3 | 2 |
| 82 | Atomistic insight into viscosity and density of silicate melts under pressure. Nature Communications, 2014, 5, 3241. | 5.8 | 133 |
| 83 | High-pressure Apparatus Integrated with Synchrotron Radiation. Reviews in Mineralogy and Geochemistry, 2014, 78, 745-777. | 2.2 | 24 |
| 84 | Sound velocity of Fe–S liquids at high pressure: Implications for the Moon's molten outer core. Earth and Planetary Science Letters, 2014, 396, 78-87. | 1.8 | 80 |
| 85 | Contrasting behavior of intermediate-range order structures in jadeite glass and melt. Physics of the Earth and Planetary Interiors, 2014, 228, 281-286. | 0.7 | 15 |
| 86 | Nanotwinned diamond with unprecedented hardness and stability. Nature, 2014, 510, 250-253. | 13.7 | 611 |
| 87 | Ponded melt at the boundary between the lithosphere and asthenosphere. Nature Geoscience, 2013, 6, 1041-1044. | 5.4 | 144 |
| 88 | Anomaly in the viscosity of liquid KCl at high pressures. Physical Review B, 2013, 87, . | 1.1 | 25 |
| 89 | Ultrahard nanotwinned cubic boron nitride. Nature, 2013, 493, 385-388. | 13.7 | 662 |
| 90 | Tian et al. reply. Nature, 2013, 502, E2-E3. | 13.7 | 10 |

| # | Article | IF | CITATIONS |
|-----|--|-----|-----------|
| 91 | Deep-Focus Earthquake Analogs Recorded at High Pressure and Temperature in the Laboratory. Science, 2013, 341, 1377-1380. | 6.0 | 120 |
| 92 | Orientation Relations During the <mml:math <br="" xmlns:mml="http://www.w3.org/1998/Math/MathML">display="inline"><mml:mi>α</mml:mi></mml:math> - <mml:math xmlns:mml="http://www.w3.org/1998/Math/MathML" display="inline"><mml:mi>Ή</mml:mi>Phase Transition of Zirconium:<i>InÂSitu</i>Texture</mml:math | 2.9 | 57 |
| 93 | Observations at High Pressure and Temperature. Physical Review Letters, 2013, 111, 195701. Highâ€pressure, highâ€temperature deformation of CaGeO ₃ (perovskite)±MgO aggregates: Implications for multiphase rheology of the lower mantle. Geochemistry, Geophysics, Geosystems, 2013, 14, 3389-3408. | 1.0 | 25 |
| 94 | Phase transitions of harzburgite and buckled slab under eastern China. Geochemistry, Geophysics, Geosystems, 2013, 14, 1182-1199. | 1.0 | 22 |
| 95 | A New Era in Mineral Physics. Eos, 2013, 94, 57-57. | 0.1 | 0 |
| 96 | A Large Volume Multi-Anvil Apparatus for the Earth Sciences Community in Taiwan. Terrestrial, Atmospheric and Oceanic Sciences, 2012, 23, 647. | 0.3 | 2 |
| 97 | Structure of jadeite melt at high pressures up to 4.9 GPa. Journal of Applied Physics, 2012, 111, 112623. | 1.1 | 39 |
| 98 | Cell assemblies for reproducible multi-anvil experiments (the COMPRES assemblies). American Mineralogist, 2012, 97, 353-368. | 0.9 | 101 |
| 99 | Texture and elastic strains in hcp-iron plastically deformed up to 17.5 GPa and 600 K: experiment and model. Modelling and Simulation in Materials Science and Engineering, 2012, 20, 024005. | 0.8 | 27 |
| 100 | Simultaneous structure and elastic wave velocity measurement of SiO2 glass at high pressures and high temperatures in a Paris-Edinburgh cell. Review of Scientific Instruments, 2012, 83, 033905. | 0.6 | 56 |
| 101 | Creep of phyllosilicates at the onset of plate tectonics. Earth and Planetary Science Letters, 2012, 345-348, 142-150. | 1.8 | 59 |
| 102 | Deformation of olivine under mantle conditions: An in situ highâ€pressure, highâ€temperature study using monochromatic synchrotron radiation. Journal of Geophysical Research, 2012, 117, . | 3.3 | 34 |
| 103 | Acoustic velocities of pure and ironâ€bearing magnesium silicate perovskite measured to 25 GPa and 1200 K. Geophysical Research Letters, 2012, 39, . | 1.5 | 45 |
| 104 | An experimental study of phase transformations in olivine under pressure and temperature conditions corresponding to the mantle transition zone. Science Bulletin, 2012, 57, 894-901. | 1.7 | 7 |
| 105 | In situ determination of the spinel-post-spinel transition in Fe3O4 at high pressure and temperature by synchrotron X-ray diffraction. American Mineralogist, 2011, 96, 820-827. | 0.9 | 13 |
| 106 | Thermal equation of state of CalrO3 post-perovskite. Physics and Chemistry of Minerals, 2011, 38, 407-417. | 0.3 | 9 |
| 107 | Combined ultrasonic elastic wave velocity and microtomography measurements at high pressures. Review of Scientific Instruments, 2011, 82, 023906. | 0.6 | 27 |
| 108 | High-pressure x-ray diffraction studies on the structure of liquid silicate using a Paris–Edinburgh type large volume press. Review of Scientific Instruments, 2011, 82, 015103. | 0.6 | 58 |

| # | Article | IF | CITATIONS |
|-----|--|-----|-----------|
| 109 | In situ high-pressure and high-temperature X-ray microtomographic imaging during large deformation: A new technique for studying mechanical behavior of multiphase composites. , 2011, 7, 40-53. | | 25 |
| 110 | Recent advances in high pressure and temperature rheological studies. Journal of Earth Science (Wuhan, China), 2010, 21, 495-516. | 1.1 | 11 |
| 111 | The thermal equation of state of FeTiO3 ilmenite based on in situ X-ray diffraction at high pressures and temperatures. American Mineralogist, 2010, 95, 1708-1716. | 0.9 | 13 |
| 112 | Recent developments in computed tomography at GSECARS. Proceedings of SPIE, 2010, , . | 0.8 | 9 |
| 113 | High-Pressure Research at the Advanced Photon Source. Synchrotron Radiation News, 2010, 23, 32-38. | 0.2 | 5 |
| 114 | Large Volume Presses for High-Pressure Studies Using Synchrotron Radiation. NATO Science for Peace and Security Series B: Physics and Biophysics, 2010, , 81-96. | 0.2 | 3 |
| 115 | Rheology at High Pressures and High Temperatures. NATO Science for Peace and Security Series B: Physics and Biophysics, 2010, , 97-110. | 0.2 | 3 |
| 116 | A combination of a Drickamer anvil apparatus and monochromatic X-rays for stress and strain measurements under high pressure. Journal of Synchrotron Radiation, 2009, 16, 742-747. | 1.0 | 7 |
| 117 | Non-cubic crystal symmetry of CaSiO3 perovskite up to 18ÂGPa and 1600ÂK. Earth and Planetary Science Letters, 2009, 282, 268-274. | 1.8 | 20 |
| 118 | High pressure effects on the iron–iron oxide and nickel–nickel oxide oxygen fugacity buffers. Earth and Planetary Science Letters, 2009, 286, 556-564. | 1.8 | 135 |
| 119 | The large-volume high-pressure facility at GSECARS: A "Swiss-army-knife―approach to synchrotron-based experimental studies. Physics of the Earth and Planetary Interiors, 2009, 174, 270-281. | 0.7 | 56 |
| 120 | Elasticity of (Mg0.87Fe0.13)2SiO4 wadsleyite to 12GPa and 1073K. Physics of the Earth and Planetary Interiors, 2009, 174, 98-104. | 0.7 | 39 |
| 121 | Volumetric properties of magnesium silicate glasses and supercooled liquid at high pressure by X-ray microtomography. Physics of the Earth and Planetary Interiors, 2009, 174, 292-301. | 0.7 | 31 |
| 122 | In situ measurement of interfacial tension of Fe–S and Fe–P liquids under high pressure using X-ray radiography and tomography techniques. Physics of the Earth and Planetary Interiors, 2009, 174, 220-226. | 0.7 | 23 |
| 123 | Advances in high-pressure mineral physics: From the deep mantle to the core. Physics of the Earth and Planetary Interiors, 2009, 174, 1-2. | 0.7 | 3 |
| 124 | Melting curve of silicon to 15GPa determined by two-dimensional angle-dispersive diffraction using a Kawai-type apparatus with X-ray transparent sintered diamond anvils. Journal of Physics and Chemistry of Solids, 2008, 69, 2255-2260. | 1.9 | 45 |
| 125 | Development of the Multi-anvil Assembly 6-6 for DIA and D-DIA type high-pressure apparatuses. High Pressure Research, 2008, 28, 307-314. | 0.4 | 73 |
| 126 | Deformation and texture development in CalrO3 post-perovskite phase up to 6ÂGPa and 1300ÂK. Earth and Planetary Science Letters, 2008, 268, 515-525. | 1.8 | 57 |

| # | Article | IF | CITATIONS |
|-----|---|-----|-----------|
| 127 | In situ investigation of high-pressure melting behavior in the Fe-S system using synchrotron X-ray radiography. High Pressure Research, 2008, 28, 315-326. | 0.4 | 14 |
| 128 | Interfacial tension measurement of Ni-S liquid using high-pressure X-ray micro-tomography. High Pressure Research, 2008, 28, 327-334. | 0.4 | 8 |
| 129 | A scanning angle energy-dispersive X-ray diffraction technique for high-pressure structure studies in diamond anvil cells. High Pressure Research, 2008, 28, 193-201. | 0.4 | 5 |
| 130 | Development of Experimental Techniques Using LVP (Large Volume Press) at GSECARS Beamlines, Advanced Photon Source. Review of High Pressure Science and Technology/Koatsuryoku No Kagaku To Gijutsu, 2008, 18, 214-222. | 0.1 | 2 |
| 131 | X-ray microtomography under high pressure. , 2007, , . | | 1 |
| 132 | High-Pressure Creep of Serpentine, Interseismic Deformation, and Initiation of Subduction. Science, 2007, 318, 1910-1913. | 6.0 | 331 |
| 133 | Rheology of É›â€iron up to 19 GPa and 600 K in the Dâ€ĐIA. Geophysical Research Letters, 2007, 34, . | 1.5 | 17 |
| 134 | DETERMINATION OF PRESSURE-DEPENDENT PHASE DIAGRAMS. , 2007, , 412-441. | | 1 |
| 135 | Recent developments in microtomography at GeoSoilEnviroCARS. , 2006, , . | | 18 |
| 136 | High-pressure cells forin situmulti-anvil experiments. High Pressure Research, 2006, 26, 283-292. | 0.4 | 21 |
| 137 | In situ X-ray diffraction study of phase transitions of FeTiO3at high pressures and temperatures using a large-volume press and synchrotron radiation. American Mineralogist, 2006, 91, 120-126. | 0.9 | 43 |
| 138 | Experimental constraints on the phase diagram of elemental zirconium. Journal of Physics and Chemistry of Solids, 2005, 66, 1213-1219. | 1.9 | 77 |
| 139 | Pressure-Induced Amorphization and Phase Transformations in Î ² -LiAlSiO4 ChemInform, 2005, 36, no. | 0.1 | 0 |
| 140 | Yield strength enhancement of MgO by nanocrystals. Journal of Materials Science, 2005, 40, 5763-5766. | 1.7 | 22 |
| 141 | Stress and strain measurements of polycrystalline materials under controlled deformation at high pressure using monochromatic synchrotron radiation. , 2005, , 137-165. | | 7 |
| 142 | High-pressure x-ray tomography microscope: Synchrotron computed microtomography at high pressure and temperature. Review of Scientific Instruments, 2005, 76, 073709. | 0.6 | 61 |
| 143 | Pressure calibration to 20GPa by simultaneous use of ultrasonic and x-ray techniques. Journal of Applied Physics, 2005, 98, 013521. | 1.1 | 33 |
| 144 | Kinetics of SiC formation during high P–T reaction between diamond and silicon. Diamond and Related Materials, 2005, 14, 1611-1615. | 1.8 | 22 |

| # | Article | IF | CITATIONS |
|-----|--|-----|-----------|
| 145 | Pressure-Induced Amorphization and Phase Transformations in \hat{I}^2 -LiAlSiO4. Chemistry of Materials, 2005, 17, 2817-2824. | 3.2 | 37 |
| 146 | Texture development and deformation mechanisms in ringwoodite. Physics of the Earth and Planetary Interiors, 2005, 152, 191-199. | 0.7 | 43 |
| 147 | In-situ elasticity measurement for the unquenchable high-pressure clinopyroxene phase: Implication for the upper mantle. Geophysical Research Letters, 2005, 32, . | 1.5 | 48 |
| 148 | Pressure and strain dependence of the strength of sintered polycrystalline Mg2SiO4ringwoodite. Geophysical Research Letters, 2005, 32, n/a-n/a. | 1.5 | 27 |
| 149 | Thermal equations of state of theα,β, andï‰phases of zirconium. Physical Review B, 2005, 71, . | 1.1 | 113 |
| 150 | Simultaneous equation of state, pressure calibration and sound velocity measurements to lower mantle pressures using multi-anvil apparatus. , 2005, , 49-66. | | 7 |
| 151 | Simultaneous equation of state, pressure calibration and sound velocity measurements to lower mantle pressures using multi-anvil apparatus. , 2005, , 49-66. | | 3 |
| 152 | High-pressure angle-dispersive powder diffraction using an energy-dispersive setup and white synchrotron radiation. , 2005, , 339-352. | | 4 |
| 153 | A new technique for angle-dispersive powder diffraction using an energy-dispersive setup and synchrotron radiation. Journal of Applied Crystallography, 2004, 37, 947-956. | 1.9 | 45 |
| 154 | Yield strength and strain hardening of MgO up to 8 GPa measured in the deformation-DIA with monochromatic X-ray diffraction. Earth and Planetary Science Letters, 2004, 226, 117-126. | 1.8 | 57 |
| 155 | Thermal equation of state of akimotoite MgSiO3 and effects of the akimotoite–garnet transformation on seismic structure near the 660 km discontinuity. Physics of the Earth and Planetary Interiors, 2004, 143-144, 57-80. | 0.7 | 24 |
| 156 | In situ measurements of sound velocities and densities across the orthopyroxene → high-pressure clinopyroxene transition in MgSiO3 at high pressure. Physics of the Earth and Planetary Interiors, 2004, 147, 27-44. | 0.7 | 106 |
| 157 | Microtomography at GeoSoilEnviroCARS. , 2004, , . | | 7 |
| 158 | High-pressure viscometry of polymerized silicate melts and limitations of the Eyring equation. American Mineralogist, 2004, 89, 1701-1708. | 0.9 | 83 |
| 159 | Flow-law for ringwoodite at subduction zone conditions. Physics of the Earth and Planetary Interiors, 2003, 136, 3-9. | 0.7 | 15 |
| 160 | The deformation-DIA: A new apparatus for high temperature triaxial deformation to pressures up to 15 GPa. Review of Scientific Instruments, 2003, 74, 3002-3011. | 0.6 | 262 |
| 161 | Viscosity and density of FeÂS liquids at high pressures. Journal of Physics Condensed Matter, 2002, 14, 11325-11330. | 0.7 | 21 |
| 162 | A large-volume press facility at the Advanced Photon Source: diffraction and imaging studies on materials relevant to the cores of planetary bodies. Journal of Physics Condensed Matter, 2002, 14, 11517-11523. | 0.7 | 23 |

| # | Article | IF | CITATIONS |
|-----|--|-----|-----------|
| 163 | Viscosity of liquid Fe at high pressure. Physical Review B, 2002, 66, . | 1.1 | 49 |
| 164 | Towards evaluating the viscosity of the Earth's outer core: An experimental high pressure study of liquid Fe-S (8.5 wt.% S). Geophysical Research Letters, 2002, 29, 58-1-58-4. | 1.5 | 52 |
| 165 | 2. New Developments in Deformation Experiments at High Pressure. , 2002, , 21-50. | | 15 |
| 166 | Laser heated diamond cell system at the Advanced Photon Source for in situ x-ray measurements at high pressure and temperature. Review of Scientific Instruments, 2001, 72, 1273. | 0.6 | 234 |
| 167 | Stability field and thermal equation of state of ε-iron determined by synchrotron X-ray diffraction in a multianvil apparatus. Journal of Geophysical Research, 2001, 106, 21799-21810. | 3.3 | 102 |
| 168 | Phase transformations: Implications for mantle structure. Geophysical Monograph Series, 2000, , 215-235. | 0.1 | 72 |
| 169 | In situ measurement of viscosity of liquids in the Fe-FeS system at high pressures and temperatures. American Mineralogist, 2000, 85, 1838-1842. | 0.9 | 101 |
| 170 | Testing plausible upper-mantle compositions using fine-scale models of the 410-km discontinuity. Geophysical Research Letters, 1999, 26, 1641-1644. | 1.5 | 28 |
| 171 | Thermal equation of state of garnets along the pyrope-majorite join. Physics of the Earth and Planetary Interiors, 1998, 105, 59-71. | 0.7 | 83 |
| 172 | Chemical- and Clapeyron-induced buoyancy at the 660 km discontinuity. Journal of Geophysical Research, 1998, 103, 7431-7441. | 3.3 | 121 |
| 173 | Advances in equation-of-state measurements in SAM-85. Geophysical Monograph Series, 1998, , 365-372. | 0.1 | 21 |
| 174 | A new facility for high-pressure research at the advanced photon source. Geophysical Monograph Series, 1998, , 79-87. | 0.1 | 11 |
| 175 | Performance of tapered anvils in a DIA-type, cubic-anvil, high-pressure apparatus for X ray diffraction studies. Geophysical Monograph Series, 1998, , 35-39. | 0.1 | 1 |
| 176 | High Brilliance and High Pressure: A New Diamond Anvil Cell Facility at the Advanced Photon Source Review of High Pressure Science and Technology/Koatsuryoku No Kagaku To Gijutsu, 1998, 7, 1529-1531. | 0.1 | 3 |
| 177 | A Multi-Anvil, High-Pressure Facility for Synchrotron Radiation Research at GeoSoilEnviroCARS at the Advanced Photon Source Review of High Pressure Science and Technology/Koatsuryoku No Kagaku To Gijutsu, 1998, 7, 1490-1495. | 0.1 | 16 |
| 178 | Yield strength, slip systems and deformation induced phase transition of San Carlos olivine up to the transition zone pressure at room temperature. Geophysical Monograph Series, 1998, , 483-493. | 0.1 | 4 |
| 179 | Rheology measurements at high pressure and temperature. Geophysical Monograph Series, 1998, , 473-482. | 0.1 | 25 |
| 180 | T-CUP: A New High-Pressure Apparatus for X-ray Studies Review of High Pressure Science and Technology/Koatsuryoku No Kagaku To Gijutsu, 1998, 7, 1520-1522. | 0.1 | 44 |

| # | Article | IF | CITATIONS |
|-----|---|-----|-----------|
| 181 | The Breakdown of Olivine to Perovskite and Magnesiowustite. Science, 1997, 275, 510-513. | 6.0 | 43 |
| 182 | Partitioning of nickel, cobalt and manganese between silicate perovskite and periclase: a test of crystal field theory at high pressure. Earth and Planetary Science Letters, 1997, 146, 499-509. | 1.8 | 20 |
| 183 | Thermoelastic equation of state of jadeiteNaAlSi2O6: An energy-dispersive Reitveld Refinement Study of low symmetry and multiple phases diffraction. Geophysical Research Letters, 1997, 24, 5-8. | 1.5 | 63 |
| 184 | Microstructures and iron partitioning in (Mg,Fe)SiO3perovskite-(Mg,Fe)O magnesiowüstite assemblages: An analytical transmission electron microscopy study. Journal of Geophysical Research, 1997, 102, 5265-5280. | 3.3 | 72 |
| 185 | Thermal equation of state of CaSiO3perovskite. Journal of Geophysical Research, 1996, 101, 661-672. | 3.3 | 177 |
| 186 | Microscopic anharmonicity and equation of state of MgSiO3-perovskite. Geophysical Research Letters, 1996, 23, 3043-3046. | 1.5 | 39 |
| 187 | Maximum solubility of FeO in (Mg, Fe)SiO3-perovskite as a function of temperature at 26 GPa: Implication for FeO content in the lower mantle. Journal of Geophysical Research, 1996, 101, 11525-11530. | 3.3 | 64 |
| 188 | Quasi-harmonic computations of thermodynamic parameters of olivines at high-pressure and high-temperature. A comparison with experiment data. Physics of the Earth and Planetary Interiors, 1996, 98, 17-29. | 0.7 | 55 |
| 189 | (??/?T) P of the lower mantle. Pure and Applied Geophysics, 1996, 146, 533-549. | 0.8 | 24 |
| 190 | (â^,Âμ/â^,T)p of the Lower Mantle. , 1996, , 533-549. | | 1 |
| 191 | Deviatoric stress measurements at high pressure and temperature. AIP Conference Proceedings, 1994, , . | 0.3 | 7 |
| 192 | Optical Absorption Spectra of (Mg, Fe)SiO3 Silicate Perovskites. Physics and Chemistry of Minerals, 1994, 20, 478. | 0.3 | 17 |
| 193 | Yield strength at high pressure and temperature. Geophysical Research Letters, 1994, 21, 753-756. | 1.5 | 157 |
| 194 | Perovskite at high P-T conditions: An in situ synchrotron X ray diffraction study of NaMgF3perovskite. Journal of Geophysical Research, 1994, 99, 2871-2885. | 3.3 | 40 |
| 195 | Thermoelasticity of CaSiO3perovskite and implications for the lower mantle. Geophysical Research Letters, 1994, 21, 895-898. | 1.5 | 54 |
| 196 | Thermodynamic properties of ferromagnesium silicate perovskites from vibrational spectroscopy. Journal of Geophysical Research, 1994, 99, 11795-11804. | 3.3 | 54 |
| 197 | P-V-T equation of state of (Mg,Fe)SiO3 perovskite: constraints on composition of the lower mantle. Physics of the Earth and Planetary Interiors, 1994, 83, 13-40. | 0.7 | 197 |
| 198 | Electron microscopy study of domain structure due to phase transitions in natural perovskite. Physics and Chemistry of Minerals, 1993, 20, 147. | 0.3 | 62 |

| # | Article | IF | CITATIONS |
|-----|--|-----|-----------|
| 199 | Determination of phase transition pressures of ZnTe under quasihydrostatic conditions. Pure and Applied Geophysics, 1993, 141, 643-652. | 0.8 | 39 |
| 200 | Electron microscopy of (Mg, Fe)SiO ₃ Perovskite: Evidence for structural phase transitions and implications for the lower mantle. Journal of Geophysical Research, 1992, 97, 12327-12347. | 3.3 | 102 |
| 201 | Phase Transition and Thermal Expansion of MgSiO3 Perovskite. Science, 1991, 251, 410-413. | 6.0 | 92 |
| 202 | Synchrotron X-ray topography studies of twinning and the phase transition at 145°C in LaGaO3 single crystals. Materials Science & Engineering A: Structural Materials: Properties, Microstructure and Processing, 1991, 132, 23-30. | 2.6 | 20 |
| 203 | High temperature transmission electron microscopy and X-ray diffraction studies of twinning and the phase transition at 145ŰC in LaGaO3. Materials Science & Engineering A: Structural Materials: Properties, Microstructure and Processing, 1991, 132, 13-21. | 2.6 | 46 |
| 204 | Phase transition in CaGeO3 perovskite: Evidence from X-ray powder diffraction, thermal expansion and heat capacity. Physics and Chemistry of Minerals, 1991, 18, 224. | 0.3 | 39 |
| 205 | Intermediate-range order in permanently densified vitreousSiO2: A neutron-diffraction and molecular-dynamics study. Physical Review B, 1991, 43, 1194-1197. | 1.1 | 274 |
| 206 | Twinning in MgSiO3 Perovskite. Science, 1990, 248, 468-471. | 6.0 | 88 |
| 207 | Crystal structure and thermal expansion of (Mg,Fe)SiO ₃ perovskite. Geophysical Research Letters, 1990, 17, 2089-2092. | 1.5 | 69 |
| 208 | Dislocation dissociation in CaGeO3 perovskite. Physics and Chemistry of Minerals, 1989, 16, 630. | 0.3 | 22 |
| 209 | Olivine as an in situ piezometer in high pressure apparatus. Physics and Chemistry of Minerals, 1988, 15, 493-497. | 0.3 | 47 |
| 210 | Orthorhombicâ€ŧetragonal phase transition in CaGeO³ perovskite at high temperature. Geophysical Research Letters, 1988, 15, 1231-1234. | 1.5 | 15 |
| 211 | Characterization of Stress, Pressure, and Temperature in SAm85, a Dia Type High Pressure Apparatus. Geophysical Monograph Series, 0, , 13-17. | 0.1 | 70 |
| 212 | Characterization of Sample Environment in a Uniaxial Split-Sphere Apparatus. Geophysical Monograph Series, 0, , 19-31. | 0.1 | 50 |